DO Note 5873-CONF

Search for Associated Higgs Boson Production with Like Sign Leptons in $p\bar{p}$ Collisions at $\sqrt{s} = 1.96$ TeV

The D0 Collaboration
URL http://www-d0.fnal.gov
(Dated: March 13, 2009)

We search for associated Higgs boson production in the process $p\bar{p} \to WH(W \to WW^*) \to \ell^{\pm}\nu\ell'^{\pm}\nu' + X$ in the ee, $e\mu$, and $\mu\mu$ channels. The search is based on data taken at the Fermilab Tevatron at $\sqrt{s} = 1.96$ TeV corresponding to 2.5 fb^{-1}. We require two like sign isolated leptons (electrons or muons) with $p_T > 15$ GeV plus additional selection cuts. No significant excess over the predicted standard model background is observed. Combining with the existing preliminary results from the previous Tevatron run period, we set 95% C.L. upper limits on $\sigma(WH) \times Br(H \to WW^*)$ between 1.04 and 0.62 pb for Higgs masses from 120 to 200 GeV at a total integrated luminosity of 3.6 fb^{-1}.

Preliminary Results for Winter 2009 Conferences

I. INTRODUCTION

In the standard model, the Higgs boson predominantly decays to a WW^* pair for Higgs boson masses above 135 GeV [1]. In fermiophobic Higgs models, the branching ratio $Br(H \rightarrow WW^*)$ may be close to 100% for Higgs masses down to ∼100 GeV [2]. Consequently, $p\bar{p} \rightarrow WH \rightarrow WWW^* \rightarrow \ell^{\pm}\nu\,\ell^{\pm}\nu' + X$ which has an easily-detected experimental signature, provides a search mechanism for both standard model and fermiphobic Higgs. The advantage of this channel over direct Higgs production, $p\bar{p} \rightarrow H \rightarrow WW^*$, is that in associated production, there are two leptons of the same electrical charge; in direct production, only opposite sign leptons are produced. The backgrounds for the same sign signature are much lower than for the opposite sign signature, where there are high rate standard model processes such as ($p\bar{p} \rightarrow Z/\gamma^*$, $p\bar{p} \rightarrow WW$, and $p\bar{p} \rightarrow t\bar{t}$. The physics background processes for the associated production process are the low rate $p\bar{p} \rightarrow WZ \rightarrow \ell\nu\ell\ell$ and $p\bar{p} \rightarrow ZZ \rightarrow \ell\ell\ell\ell$. The non-resonant triple vector boson production (VVV, $V = W, Z$) and the production of $t\bar{t} + V$ are negligibly small.

As there are two neutrinos in the final state, complete reconstruction of the Higgs mass in the candidate events is not feasible. A potential Higgs boson signal would appear as an excess in the number of observed events with two like sign leptons and certain kinematic properties resulting from the two neutrinos. In the absence of an excess over the expected number of events from background processes, upper cross section limits are set. These limits vary with the Higgs mass in the range of 120 to 200 GeV.

There are two instrumental backgrounds. The first, "charge flips", originates from the misreconstruction of the charge of one of the leptons. For the same lepton flavor channels (ee and $\mu\mu$) this background has the underlying physics of the Drell-Yan process, $p\bar{p} \rightarrow Z/\gamma^* \rightarrow \ell^+\ell^-$. When the two leptons are of different flavor, this background is negligible. The second instrumental background is jets from QCD produced multijet events. The jets may be falsely identified for a number of reasons as isolated leptons with high momenta transverse to the axis of the $p\bar{p}$ collision (p_T).

II. THE DØ DETECTOR

The DØ detector has a central-tracking system, calorimeters, and a muon spectrometer [3]. The central tracking system includes a silicon microstrip tracker (SMT) and a central fiber tracker (CFT) embedded in 2 T solenoidal magnetic field, and provides tracking in the pseudorapidity range of $|\eta| < 3$. The uranium/liquid argon calorimeter consists of a central section (CC) covering pseudorapidities η up to ≈ 1.1, and two end calorimeters (EC) that extend coverage to $\eta \approx 4.2$. The muon detection system surrounds the calorimeters and allows for detection of muons at pseudorapidities $|\eta| < 2$. It is a toroidal spectrometer and provides a second measurement of p_T and hence, electrical charge. Timing information is recorded in the muon system and is used to veto activity from cosmic rays. Luminosity is measured from the $p\bar{p}$ inelastic collision rate using plastic scintillator arrays.

III. DATA AND MONTE CARLO SAMPLES

This analysis uses data collected by the DØ experiment between June 2006 and September 2008. The data samples correspond to total integrated luminosities of 2.5 fb^{-1} after applying data quality requirements.

The signal and background processes were generated with PYTHIA version 6.323 [4] using CTEQ6L1 parton density functions and with a detailed GEANT 3 based [5] simulation of the DØ detector. The signal cross section was calculated at NLO using HDECAY [6] and HIGLU [7]. A further NNLO correction factor of 0.96 was applied. The diboson production cross sections were taken to be the values recommended by the Tevatron New Phenomena and Higgs Working Group [8].

The Monte Carlo samples are normalized to theoretical cross sections multiplied by the integrated luminosity of the data samples, with an additional corrections to account for the event reconstruction and selection efficiencies. These factors are obtained by normalizing the number of unlike-sign events in the $Z \rightarrow \ell\ell$ peak. The Z/$\gamma*$ cross section is calculated with CTEQ6.1M PDFs using the NNLO to LO K-factor according to [9].

IV. EVENT SELECTION

The analysis starts with the selection of events that have at least two candidate leptons, which can be either electrons or muons. There is no explicit trigger requirement applied, however, most events are collected by the single lepton or double lepton triggers.

For electrons, we require a cluster of electromagnetic (EM) energy in the central calorimeter region ($|\eta| < 1.1$) with $p_T > 15$ GeV, matched to a track in the central tracker. The electron energy is reconstructed in a cone of radius, $\mathcal{R} = 0.2$, where $\mathcal{R} = \sqrt{(\Delta\eta)^2 + (\Delta\phi)^2}$ and ϕ is the azimuthal angle. The electromagnetic energy fraction is required to be greater than 0.9, and the isolation fraction less than 0.2, where the isolation fraction is defined as the ratio of the calorimeter deposition in the annulus between radii, $0.2 < \mathcal{R} < 0.4$, to the electron energy. These electrons are called "loose" and are used to estimate the multijet background. The signal search proceeds with electrons that further pass a cut on calorimeter energy over track momentum, $E/p < 3$, and also pass a cut on an eight variable likelihood variable that selects isolated prompt electrons. These are called "tight" electrons.

For muons, we require muon spectrometer activity that passes cosmic ray veto timing cuts and which again matches a $p_T > 15$ GeV track in the central tracker. The reconstructed pseudorapidity must satisfy $|\eta| < 1.8$ and to reduce charge flip backgrounds, the constraint $p_T < 200$ GeV is applied. Requiring that the track emanates from the primary interaction point improves the purity of this "loose" muon sample, as does the requirement that the track also does not match an EM cluster and be separated from identified jets by more than $\Delta\mathcal{R} = 0.1$. The sum of energy in the calorimeter within a hollow cone $0.1 < \mathcal{R} < 0.4$ around the track $\sum_{0.1<\mathcal{R}<0.4} E_T^{cell}$ must be less than 2.5 GeV, and the sum of p_T of all tracks in the cone $\mathcal{R} < 0.5$ around the muon's track $\sum_{\mathcal{R}<0.5} p_T^{trk}$ also must be less than 2.5 GeV.

An additional set of track quality cuts, aimed at reducing the charge flip background are applied to the tight lepton samples. These include requirements on the maximum distance in the direction of the $p\bar{p}$ collision axis between the lepton tracks and the vertex (1 cm), a maximum distance of closest approach to the primary vertex $dca < 0.02$ cm and its significance $|dca/\sigma(dca)| < 3$, $\chi^2/NDF < 4$ for the lepton track fit, and a minimum number of SMT and CFT measurements of 3 and 12 respectively.

The selected events are required to have the dilepton invariant mass $m_{\ell\ell} > 30$ GeV and both leptons are required to come from the primary vertex and have the same charge. We veto events with a third high p_T lepton.

The efficiency of the lepton selection (trigger, lepton quality and track quality cuts) and the third lepton veto in Monte Carlo samples are corrected by the scale factors explained in Section III.

V. BACKGROUNDS

The physics background (true like sign isolated high p_T leptons) is primarily from $p\bar{p} \to WZ \to \ \ell^{\pm}\nu\ell^{\pm}\ell^{\mp}$, where the two same sign leptons were found and the unlike sign lepton was not. The contribution from $p\bar{p} \to ZZ \to \ \ell^{\pm}\ell^{\mp}\ell^{\pm}\ell^{\mp}$, where two leptons were not identified is smaller, as the production rate is lower:

$$p\bar{p} \to WZ \ \ \sigma = 3.45 \pm 0.24 \ pb$$
$$p\bar{p} \to ZZ \ \ \sigma = 1.37 \pm 0.10 \ pb$$

This background is estimated from the known cross sections, and branching ratios of Z and W boson decays, and allowing for event selection efficiency obtained from Monte Carlo samples.

The instrumental backgrounds are considerably larger than the physics backgrounds. The charge flip background, created by the misreconstruction of the charge of one of the leptons, is mostly from the Drell-Yan process. However, other processes such as $WW \to \ \ell^{\pm}\nu\ell^{\mp}\nu$ and $t\bar{t} \to \ \ell^{\pm}\ell^{\mp} + X$ will contribute a small fraction of this background. The multijet background, in the case of jets misidentified as muons, contains muons from semileptonic heavy flavor or tau decays, punch-through hadrons misidentified as muons, and muons from pion or kaon decays in flight. In the case of jets misidentified as electrons, the multijet background contains electrons from semileptonic heavy flavor decays, from hadrons misidentified as electrons, and from γ conversions. A small component of $t\bar{t} \to \ \ell^{\pm} + X$ will contribute to multijet background if a jet is misidentified as a lepton. Similarly, $p\bar{p} \to W + jets$ will contribute to the multijet background. These last two cases are strongly suppressed by the small cross section to produce top or vector bosons relative to the cross sections for quantum chromodynamic processes.

No attempt is made to calculate rates for instrumental backgrounds from known cross sections and detector simulation, as such a calculation is not expected to be reliable. Instead, these rates are measured in the data.

The contribution from the charge flips in $\mu\mu$ events is estimated using two measurements of the same charge. The first one is the measurement of the track charge in the central tracker, and the second measurement called the "local" muon charge as measured by the muon spectrometer. The second measurement is of much lower reliability than the first measurement. The fraction of the charge flips is derived from the number of events where the two measurements give the same answer for both leptons (SS), agree for one lepton and disagree for another one (OS), or disagree for both leptons (OO). The expected number of events in these three categories depends on the fraction of the $\mu\mu$ sample that are charge flip events, and on the marginal efficiency of the local charge measurement. The marginal efficiency is found from unlike sign $Z \to \ \mu\mu$ events and parameterized as a function of $1/p_T$. The expected number of events consequently depends only on the charge flip fraction, and that may be adjusted so that the expectation matches the observation.

The contribution of the charge flips in ee events is obtained by multiplying the charge flip rate (that is, the ratio of like sign to either sign dilepton events) by the number of either sign dilepton events in data. The charge flip rate and the product with the number of either sign dilepton events in the data are parameterized with the p_T of that lepton which has the largest p_T in the event. The charge flip rate is first derived using Monte Carlo $Z \rightarrow e^+e^-$ events over the full range of p_T values for which adequate statistics are available (15 to 200 GeV). It is then scaled by the ratio of rates in data *vs.* Monte Carlo in the region 85 GeV $< m_{ee} <$ 100 GeV, where the charge flip contribution in like sign events is assumed to be 100%.

The fraction of charge flips in the $e\mu$ channel is negligible as the direct Drell-Yan process $p\bar{p} \rightarrow Z/\gamma* \rightarrow \ell^+\ell^-$ does not exist. The charge flip contamination from $Z/\gamma* \rightarrow \tau^+\tau^- \rightarrow \ell^+\ell^-$ is suppressed by the branching fraction of the tau into electrons and muons. In addition, leptons from τ decays have lower p_T, so fewer of them pass the 15 GeV p_T cut, and those that do have a lower charge flip fraction. An upper limit on the contribution from the Drell-Yan production of τ pairs may be obtained from the product of the average electron and muon charge flip rates referenced to the number of loose tagged events (~ 0.007) with the number of loose tagged $e\mu$ events times the $\tau \rightarrow e\nu\nu$ and $\tau \rightarrow \mu\nu\nu$ branching ratios. This is about 1/4 of an event, and this estimate does not account for the different p_T spectrum from τ events.

The fraction of like sign events due to multijet may be calculated from the fraction of events without tight leptons (N_0) and with exactly one tight lepton (N_1). Assuming that these samples consist mostly of fake leptons which have probability ε_Q to be identified as tight,

$$\begin{aligned} N_0 &= (1-\varepsilon_Q)^2 \\ N_1 &= 2\varepsilon_Q(1-\varepsilon_Q) \\ N_Q &= \varepsilon_Q^2. \end{aligned} \tag{1}$$

Consequently, $N_Q = \varepsilon_Q^2 = N_1^2/4N_0$. Once this fraction has been obtained, it is multiplied by the total number of events with 2 leptons that pass the loose-tagging criteria. The actual number of events with two tight-tagged leptons may differ from this result, because of sources of leptons other than multijet backgrounds, including signal.

The assumption that these samples consist of fake leptons is the primary limitation of this method. The like sign sample, even with loose tags, can contain true leptons from $Z/\gamma^* \rightarrow \mu^+\mu^-$ where one of the μ charges is incorrectly reconstructed. This contamination will increase the measured value of ε_Q.

To address this contamination issue, we compute ε_Q in different $m_{\ell\ell}$ bins: 30 - 50 GeV, 50 - 70 GeV, 70 - 110 GeV and 110 - 300 GeV, and select the lowest value of ε_Q found. Then we assign a systematic uncertainty to allow for any residual contamination. The systematic uncertainty is the lesser of (a) the difference between the lowest and the second lowest value of ε_Q and (b) the difference between the lowest and the mean value of ε_Q obtained without binning. In the ee case, ε_Q is $11.9 \pm 1.5 \pm 0.4\%$ at the final selection; for $\mu\mu$, it is $6.0 \pm 0.8 \pm 1.8\%$.

A second potential issue is possible correlations between the tagging of one jet as a lepton and the tagging of a second jet as a lepton. The data may be used to estimate the correlation coefficient, but only under the assumption that there is no contamination in the sample. We take that estimate to set the range of possible variation of the correlation coefficient from zero. The resulting changes in the estimated level of multijet backgrounds is taken as a systematic uncertainty.

The number of multijet events in the $e\mu$ sample is estimated using the sample with a tight muon and any electron. The distribution of the eight variable likelihood variable for EM clusters is fitted using templates for true and fake electrons. The true electron likelihood distribution was taken from events in the opposite sign data at the Z resonance. The likelihood distribution for jets faking electrons was taken from events in the same sign ee sample, with reconstructed dilepton mass in the 30-70 GeV range.

VI. EVENT SAMPLE COMPOSITION

The number of predicted and observed events after all selections is summarized in Table I and Table II. In all channels, the observed number of events is in agreement with the predicted background. As an example, Figure 1 shows the dilepton invariant mass distributions for the three channels before and after track quality cuts.

The diboson background is taken from Monte Carlo samples, normalized to the integrated luminosity of 2.5 fb^{-1}, with detection efficiency corrections applied. For the charge flip background distributions in ee channel data with either lepton charge combination, scaled by the charge flip rate as described in Section V was used. For $\mu\mu$ channel where the magnitude of the track momentum for the flipped muon is mismeasured, Monte Carlo $Z \rightarrow \mu\mu$ sample is used to model the distributions. Since the sample statistics are limited, the shape before track quality cuts is retained through to the final selection, normalized to the number of charge flip events estimated from the local charge measurement as described in Section V. The multijet distributions for the $\mu\mu$ channel is modeled by inverting the

isolation requirement on both muons. For the ee channel the electron likelihood cut is inverted and E/p cut is removed. Finally, for $e\mu$ channel, either the electron likelihood cut or the muon isolation cuts (or both) are inverted.

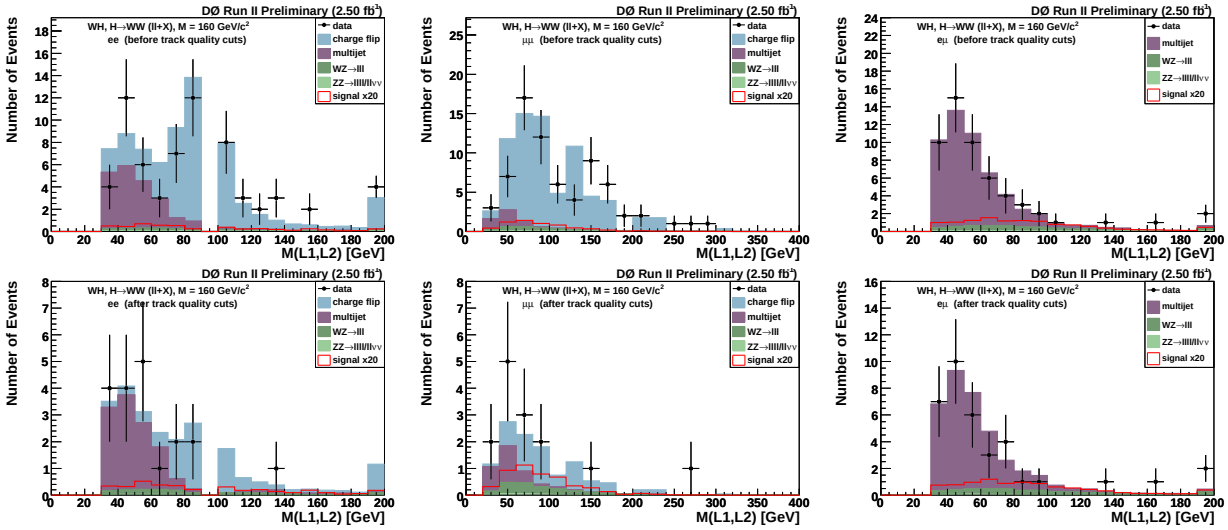

FIG. 1: The distribution of dilepton invariant mass in the ee (left), $\mu\mu$ (middle), and $e\mu$ (right) channel before track quality cuts (top row) and after all selection cuts (bottom row).

VII. MULTIVARIATE METHOD

After selection of events with high p_T same sign lepton pairs, and understanding the background contributions as described above, we construct a variable to separate the signal from the major backgrounds. This likelihood based discriminant is used in the final limit calculation. For the ee and $\mu\mu$ case, discriminants to separate signal from charge flip backgrounds were found to be effective at separating signal from multijet backgrounds, and so only one of the two discriminants that were created were actually used. In the $e\mu$ channel, where there is no substantial charge flip background, only an anti-multijet discriminant is used. We have not devised good discriminants against the diboson backgrounds, but the charge-flip and multijet backgrounds are much larger than the diboson backgrounds.

The `TMVA` package [10] was used to construct, test, and implement the discriminants. We found that good results were obtained using the PDE-RS algorithm [11], which is a multidimensional likelihood estimator. The best results occurred with the use of the "Adaptive Volume" option with a Gaussian `KernelEstimator` of `GaussSigma` = 0.3 option is used. The construction of the discriminant allows for individual event weights, and these are scaled to allow for the different effective luminosity of the different Monte Carlo samples.

Our discriminant testing and training samples are:

- Charge-flip: From $Z/\gamma^* \to \ell^+\ell^-$ Monte Carlo, we select events with reconstructed opposite sign dileptons before track quality cuts.
- Multijet: From the data, we use same sign events at least one lepton passing the loose but not the tight selection criteria. For the ee sample, contamination from charge flip events into the multijet sample is reduced by requiring $m_{ee} < 80$ GeV. Track quality cuts are not applied.
- Signal: Same sign Monte Carlo events before track quality cuts are used. To date, only $M_H = 160$ GeV events have been used.

One-half of the events in each sample are used to define the discriminants and the other half are used to understand their performance. We test for overtraining by making sure that the half of the events not used in defining the discriminant are distributed in the discriminant's output variable in the same way as the events that were used to define the discriminant.

If the training sample is not orthogonal to the events used to model the background it is in principle possible that the training sample might have a systematically lower discriminant value because of overtraining. Although we do

TABLE I: The number of predicted and observed events before and after the track quality cuts. The signal event yields are based on the standard model Higgs boson production cross section and the decay branching ratio. For the ee channel, the control region used to parameterize the charge flip rate is excluded. Statistical and systematic uncertainties have been combined.

	ee channel		$\mu\mu$ channel		$e\mu$ channel	
	preselection	final	preselection	final	preselection	final
$WZ \to \ell\nu\ell\ell$	2.41 ± 0.17	1.76 ± 0.12	3.27 ± 0.23	2.42 ± 0.17	6.99 ± 0.49	5.18 ± 0.36
$ZZ \to \ell\ell\ell\ell$	0.53 ± 0.04	0.37 ± 0.03	0.58 ± 0.04	0.43 ± 0.03	1.17 ± 0.08	0.87 ± 0.06
multijet	20.2 ± 10.2	11.8 ± 11.2	4.4 ± 5.0	3.0 ± 4.2	48.5 ± 4.4	33.2 ± 3.0
charge flip	49.2 ± 7.4	9.7 ± 5.8	65.2 ± 6.5	6.5 ± 6.7	- ± -	- ± -
total background	72.3 ± 12.6	23.6 ± 12.6	73.5 ± 8.2	12.3 ± 7.9	56.7 ± 4.4	39.2 ± 3.0
data	66	19	71	14	54	35
$WH(160) \to \ell\ell jj$	0.137	0.101	0.164	0.128	0.334	0.255
$WH(160) \to \ell\ell\ell$	0.047	0.035	0.069	0.055	0.129	0.098

TABLE II: The number of predicted signal events before and after the track quality cuts for different assumed Higgs boson masses. The event yields are based on the standard model Higgs boson production cross section and the decay branching ratio. For the ee channel, the control region used to parameterize the charge flip rate is excluded. Statistical and systematic uncertainties have been combined.

	ee channel		$\mu\mu$ channel		$e\mu$ channel	
	preselection	final	preselection	final	preselection	final
$WH(120) \to \ell\ell jj$	0.041	0.030	0.066	0.051	0.108	0.084
$WH(120) \to \ell\ell\ell$	0.020	0.014	0.027	0.021	0.052	0.040
$WH(140) \to \ell\ell jj$	0.100	0.072	0.152	0.120	0.285	0.212
$WH(140) \to \ell\ell\ell$	0.040	0.029	0.057	0.046	0.123	0.095
$WH(180) \to \ell\ell jj$	0.082	0.059	0.113	0.086	0.230	0.177
$WH(180) \to \ell\ell\ell$	0.034	0.025	0.043	0.034	0.083	0.063
$WH(200) \to \ell\ell jj$	0.047	0.035	0.062	0.048	0.132	0.098
$WH(200) \to \ell\ell\ell$	0.018	0.013	0.024	0.019	0.043	0.033

not see overtraining, we take the precaution of dividing the multijet and signal samples in half and repeating the training with half of the events while using the other half of the events to produce the background shape distributions of section VI.

The variables used are:

- If the mode contains electrons, we use $\not\!\!E_T$, the magnitude of the missing momentum in the transverse plane
- If the discriminant is against multijet, we use the minimum p_T of the two leptons
- If the mode contains muons, we use $\Delta\phi$, the angle between the two leptons, as projected onto the transverse plane
- If the mode contains muons, we use $\perp MET\mu$, defined below

This prescription results in a single variable for the discriminant to separate signal from charge flip backgrounds in the ee case. We just use that variable, $\not\!\!E_T$, in lieu of a discriminant in that case.

The variable $\perp MET\mu$ is designed to try to capture information about $\not\!\!E_T$ that is not due to mismeasurement of muon momenta. The muon that is closest to $\not\!\!E_T$ in the transverse plane is found, where "closest" refers to the opening angle to either the muon momentum or to its opposite, as seen in the transverse plane. Then the component of $\not\!\!E_T$ that is perpendicular to the muon momentum is used.

Figures 2 and 3 show the distribution of the input variables.

Figure 4 shows the multivariate discriminant distributions for data and the sum of the backgrounds in ee, $\mu\mu$ and $e\mu$ channels respectively.

VIII. RESULTS

In absence of an excess in the number of observed events over the standard model background, cross section upper limits have been calculated using the modified frequentist approach [12]. The results of these calculations are

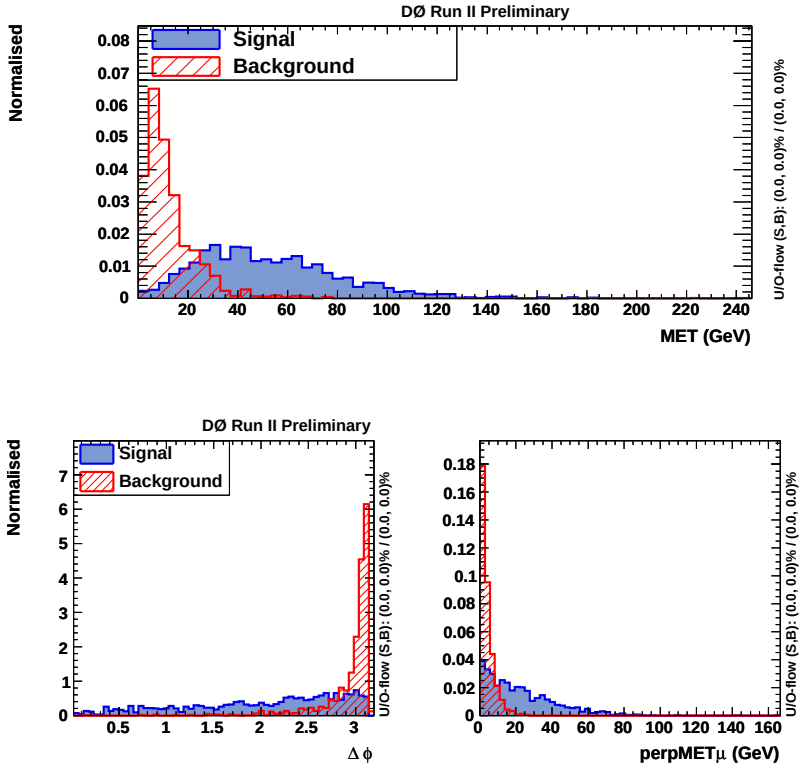

FIG. 2: Distributions of the signal (Higgs boson mass = 160 GeV) and background variables used in the discriminants against charge flipped Drell Yan background. Top: for the ee mode; Bottom: for the $\mu\mu$ mode.

summarized in Table III and IV. Preliminary results from the previous Tevatron run period [13] are combined to give a cross section limit at a total integrated luminosity of approximately 3.6 fb^{-1}. Fig. 5 show the observed an exected cross section limits as the ratio to the standard model cross section and the log likelihoood ratio (LLR) as a function of the Higgs boson mass. Fig. 6 shows the observed and expected upper limits on $\sigma(WH) \times Br(H \rightarrow WW^*)$ together with the theoretical prediction for the standard model, the theoretical prediction for a fermiophobic Higgs, the published DØ results obtained with 0.4 fb^{-1} [14], and the CDF Run II results obtained with 2.7 fb^{-1} [15]. The main source of systematic uncertainty is uncertainty on instrumental background: 94.9% in ee, 142.4% in $\mu\mu$ and 9.0% in $e\mu$ on the QCD events, 59.8% on the number of charge flips in the ee channel, 103.2% on the number of charge flips in the $\mu\mu$ channel at final selection. Other sources of uncertainty include luminosity, lepton ID, and physics background cross section.

IX. CONCLUSIONS

A search has been performed on the process $p\bar{p} \rightarrow WH \rightarrow WWW^* \rightarrow \ell^{\pm}\nu\ell'^{\pm}\nu' + X$ in the ee, $e\mu$ and $\mu\mu$ channels. After the final selection, 29 events in the ee channel, 19 events in the $e\mu$ channel, and 12 events in the $\mu\mu$ channel have been observed in agreement with the predicted standard model background. The expected (observed) upper limits on $\sigma(WH) \times Br(H \rightarrow WW^*)$ for the combination of all three channels at the total integrated luminosity of 3.6 fb^{-1} including the results from the previous run period are found to be between 0.65 (1.04) and 0.35 (0.62) pb for Higgs boson masses from 120 to 200 GeV.

Acknowledgments

We thank the staffs at Fermilab and collaborating institutions, and acknowledge support from the DOE and NSF (USA); CEA and CNRS/IN2P3 (France); FASI, Rosatom and RFBR (Russia); CAPES, CNPq, FAPERJ, FAPESP and FUNDUNESP (Brazil); DAE and DST (India); Colciencias (Colombia); CONACyT (Mexico); KRF and KOSEF

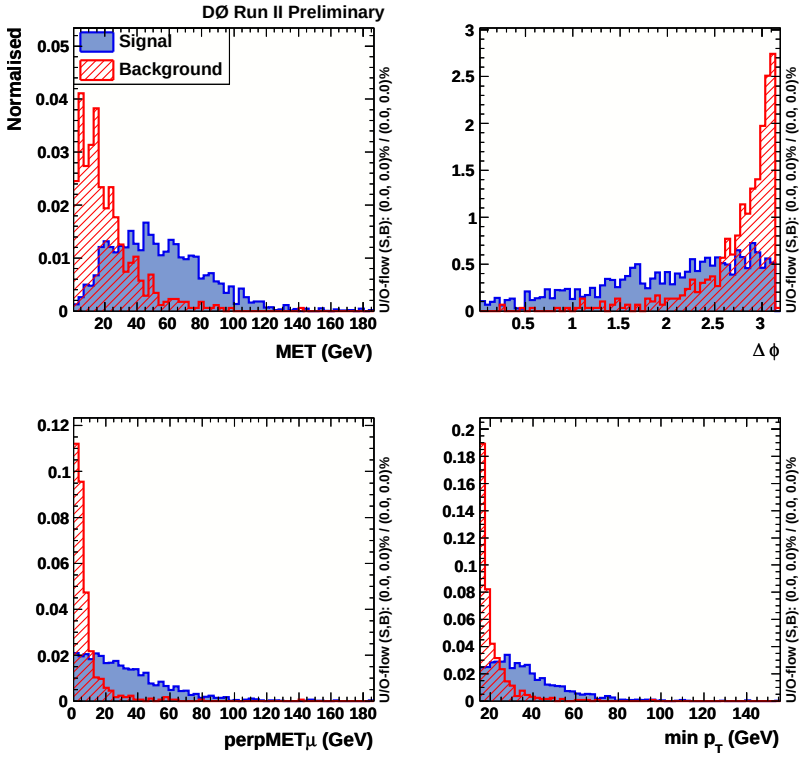

FIG. 3: Distributions of the signal and background variables used in the multivariate discriminant against multijet background in the $e\mu$ mode.

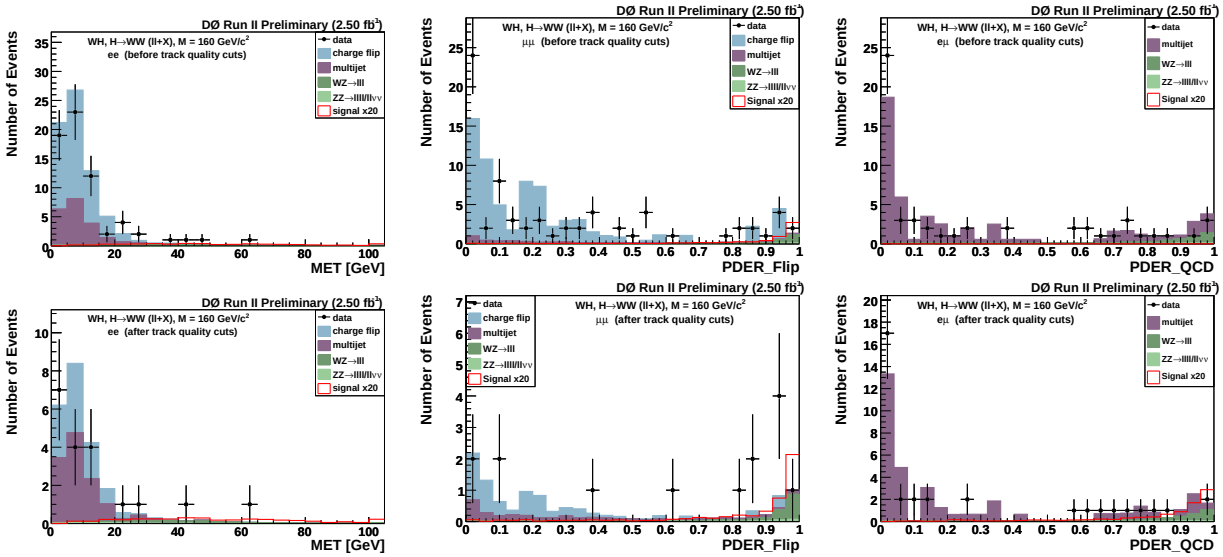

FIG. 4: The distribution of the missing E_T in ee channel (left) and the multivariate discriminant against charge flip in $\mu\mu$ channel (middle), and the discriminant trained against multijet background in $e\mu$ channel (right), before track quality cuts (top row) and after all selection cuts (bottom row).

(Korea); CONICET and UBACyT (Argentina); FOM (The Netherlands); PPARC (United Kingdom); MSMT (Czech Republic); CRC Program, CFI, NSERC and WestGrid Project (Canada); BMBF and DFG (Germany); SFI (Ireland);

TABLE III: The expected(observed) production cross section limits (pb) for individual channels and for the combination.

m_H (GeV)	120	140	160	180	200
ee	2.64 (3.46)	2.21 (2.89)	1.78 (2.37)	1.77 (2.35)	1.51 (2.03)
$\mu\mu$	1.98 (3.95)	1.71 (3.54)	1.65 (3.40)	1.57 (3.17)	1.53 (2.72)
$e\mu$	1.39 (1.47)	1.11 (1.13)	1.00 (1.04)	0.88 (0.90)	0.78 (0.79)
Run IIb combined	0.95 (1.61)	0.78 (1.31)	0.70 (1.18)	0.64 (1.04)	0.56 (0.90)
Run IIa + IIb	0.65 (1.04)	0.55 (0.91)	0.49 (0.84)	0.42 (0.73)	0.35 (0.62)

TABLE IV: The expected(observed) production cross section limits in terms of the ratio to the standard model cross section for individual channels and for the combination.

m_H (GeV)	120	140	160	180	200
ee	130.7 (170.9)	52.8 (69.0)	38.7 (51.5)	61.7 (81.9)	105.6 (142.0)
$\mu\mu$	97.9 (195.5)	40.8 (84.6)	35.8 (73.9)	54.5 (110.4)	93.0 (189.7)
$e\mu$	68.9 (72.9)	26.4 (27.1)	21.8 (22.7)	30.8 (31.5)	54.8 (55.1)
Run IIb combined	47.0 (79.9)	18.6 (31.3)	15.1 (25.6)	22.2 (36.3)	39.0 (63.2)
Run IIa + IIb	32.2 (51.6)	13.2 (21.7)	10.7 (18.4)	14.6 (25.5)	24.4 (43.0)

Research Corporation, Alexander von Humboldt Foundation, and the Marie Curie Program.

[1] M. Spira, in Proceedings for "Physics at Run II: Workshop on Supersymmetry / Higgs", 19-21 Nov 1998, Batavia IL U.S.A., arXiv:hep-ph/9810289 (1998).
[2] L. Brucher and R. Santos, Eur. Phys. J. C **12**, 87 (2000).
[3] V. M. Abazov *et al.*, (DØ Collaboration), Nucl. Instrum. Methods Phys. Res. A **565**, 463 (2006).
[4] T. Sjöstrand *et al.*, Comp. Phys. Comm. **135**, 238 (2001).
[5] CERN Program Library, `http://wwwasd.cern.ch/wwwasd/cernlib`.
[6] A. Djouadi *et al.*, Comp. Phys. Comm. **108**, 56 (1998).
[7] M. Spira, arXiv:hep-ph/9510347 (1995).
[8] The TEVNPH Working Group (The CDF and DØ Collaborations), FERMILAB-PUB-09-060-E and `http://tevnphwg.fnal.gov`; see also J. M. Campbell and R. K. Ellis, Phys. Rev. D **60**, 113006 (1999).
[9] R. Hamberg, W. L. van Neerven, and T. Matsuura, Nucl. Phys. **B359**, 343 (1991) [Erratum-ibid. **B644**, 403 (2002)].
[10] `http://tmva.sourceforge.net`
[11] T. Carli and B. Koblitz, Nucl. Instrum. Methods A **501**, 576 (2003).
[12] T. Junk, Nucl. Instrum. Methods A **434**, 435 (1999).
[13] DØ Collaboration, DØ Conference Note 5485 (2007).
[14] V. M. Abazov *et al.*, (DØ Collaboration), Phys. Rev. Lett. **97**, 151804 (2006).
[15] T. Aaltonen *et al.*, (The CDF Collaboration),CDF/ANAL/EXOTIC/PUBLIC/7307 (2008).

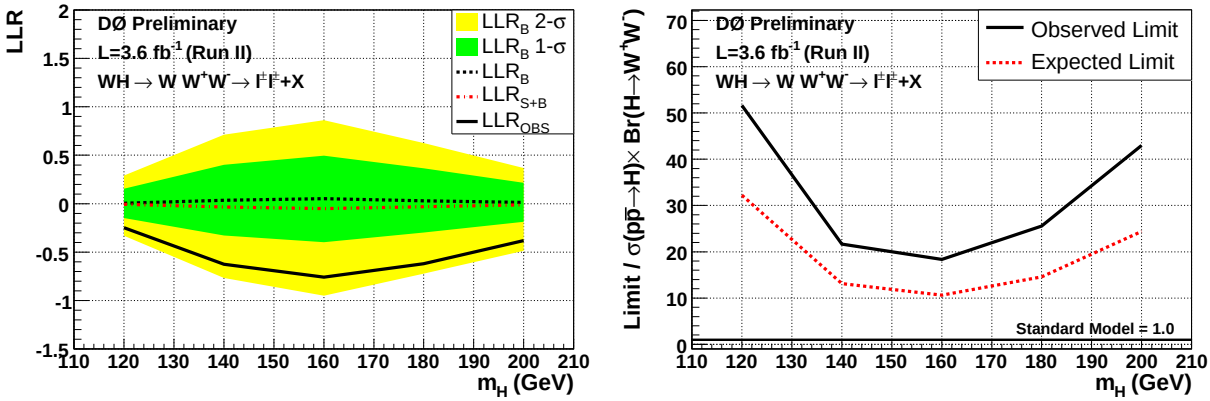

FIG. 5: Right: the logarithmic likelihood ratios (LLR) for the tree channels combined at 3.6 fb^{-1}. Lower dashed line: LLR for the signal + background hypothesis; upper dashed line: LLR for the background-only hypothesis; full line: observed data; green (yellow) bands: 1 (2) standard deviation for background-only LLR. Right: expected and observed upper limits on $\sigma(WH) \times Br(H \to WW^*)$ at the 95% confidence level, as a ratio to the standard model cross section.

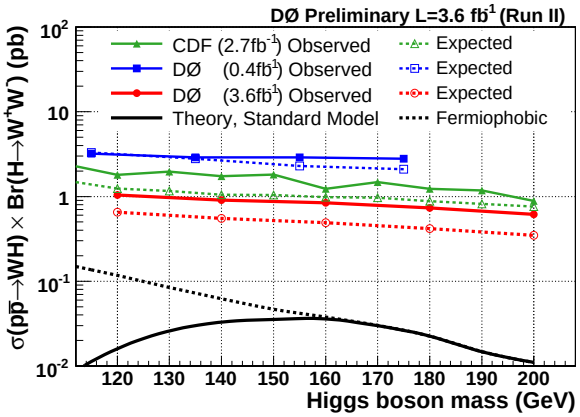

FIG. 6: The expected and observed upper limits on $\sigma(WH) \times Br(H \to WW^*)$ at the 95% confidence level, in pb. Also shown are the previous DØ result obtained with 0.4 fb^{-1}, the CDF Run II result obtained with 2.7 fb^{-1}, and theoretical predictions.